

# $B_s \rightarrow \phi l^+ l^-$ decays in the topcolor-assisted technicolor model

Lin-Xia Lü<sup>1a</sup>, Xing-qiang Yang<sup>1</sup>, and Zong-chang Wang<sup>1</sup>

<sup>1</sup> *Physics and electronic engineering college, Nanyang Normal University,  
Nanyang, Henan 473061, P.R. China*

## Abstract

Using the updated form factors within the light-cone QCD sum rule approach, we calculate the new physics contributions to rare semileptonic  $\bar{B}_s \rightarrow \phi \mu^+ \mu^-$ ,  $\phi \tau^+ \tau^-$  decays from the new particles appearing in the topcolor-assisted technicolor (TC2) model. In our evaluations, we find that: (i) the branching ratio, normalized forward-backward asymmetry and lepton polarization asymmetries show highly sensitivity to charged top-pions contributions and little sensitivity to  $Z'$  contributions. The TC2 enhancements to the branching ratios of these decays can reach a factor of  $\sim 2$ ; (ii) the NP enhancement to the forward-backward asymmetry of the decay  $B_s \rightarrow \phi \mu^+ \mu^-$  is in the range  $-13\%$  to  $3\%$ , but  $-9\%$  to  $-6\%$  for decay  $B_s \rightarrow \phi \tau^+ \tau^-$  compared to the SM predictions; (iii) the TC2 model provide an enhancement of about  $12\%$  to the longitudinal polarization asymmetry  $P_L$  for decay  $B_s \rightarrow \phi \mu^+ \mu^-$ , but a decrease of about  $10\%$  to the transverse polarization asymmetry  $P_T$  for the decay  $B_s \rightarrow \phi \tau^+ \tau^-$ .

PACS numbers: 13.20.He, 12.15.Ji, 12.60.Nz, 14.40.Nd

---

<sup>a</sup> E-mail: lvlinxia@sina.com

## I. INTRODUCTION

High energy physics experiments are designed to resolve the yet-unanswered questions in the Standard Model (SM) through searches of new physics (NP) using two approaches: high energy or high luminosity approach. The first approach is to use high energy collider to produce and discover new particles directly. The second one is to measure flavor physics observables at for example B factory experiments and search for the signal or evidence of a deviation from the SM prediction. A natural place is to investigate the flavor-changing neutral current (FCNC) processes in B meson rare decays. In the SM, the rare B decays are all induced by the so-called box and/or penguin diagrams. Since these rare decay modes are highly suppressed in the SM, they may serve as a good hunting ground for testing the SM and probing possible NP effects.

At the quark level, the decays  $B_s \rightarrow \phi l^+ l^-$  proceed via FCNC transition  $b \rightarrow sl^+ l^-$ . The decays  $B_s \rightarrow \phi l^+ l^-$  will be one of the most important rare decays to be studied at the LHCb experiment and other B physics experiments. The theoretically predicted branching ratio has the value of  $\sim 1.65 \times 10^{-6}$  for the  $B_s \rightarrow \phi \mu^+ \mu^-$  mode [1]. The experimental observation was first done by CDF collaboration [2] and the updated branching fraction is [3]

$$\mathcal{B}(\bar{B}_s \rightarrow \phi \mu^+ \mu^-) = [1.47 \pm 0.24(\text{stat.}) \pm 0.46(\text{syst.})] \times 10^{-6}. \quad (1)$$

which is consistent with the SM prediction. However, the experimental errors are still large and this decay allow for sizable NP contributions. We will evaluate the effects of possible NP in these decays in the topcolor-assisted model.

The decays  $B_s \rightarrow \phi l^+ l^-$  have been studied by employing the low-energy effective Hamiltonian and nonperturbative approaches to compute the decay form factors in the framework of the SM [1, 4]. Many studies about possible new physics contributions to these decays induced by loop diagrams involving various new particles have been published, for example, in the two Higgs doublet model [5], the universal extra dimension scenario [6], the family non-universal  $Z'$  model [7] and other new physics scenarios [8].

The topcolor-assisted (TC2) [9] model is one of the important candidates for a mechanism of natural electroweak symmetry breaking. In the TC2 model, the non-universal gauge boson  $Z'$ , top-pions  $\pi_t^{0,\pm}$ , top-Higgs boson  $h_t^0$  and other bound states may provide potentially large loop effects on low energy observables. In this paper, we will investigate the new contributions from the new particles predicted by the TC2 model to the branching ratios, the forward-backward asymmetry, and double lepton polarization of the decays  $B_s \rightarrow \phi l^+ l^-$ .

The paper is arranged as follows. In Section II, we give a brief review of the topcolor-

assisted technicolor model. In Section III, we present the theoretical framework for  $B_s \rightarrow \phi l^+ l^-$  decays within the SM and the TC2 model, then give the definitions and the derivations of the form factors in the decays  $B_s \rightarrow \phi l^+ l^-$  using the updated form factors within the light-cone QCD sum rule. In Section IV, we introduce the basic formula for experimental observables, including dilepton invariant mass spectrum, forward-backward asymmetry (FBA), and lepton polarization. In Section V, we present our numerical results for these decays in the SM and the TC2 model. The conclusions are presented in the final section.

## II. OUTLINE OF THE TC2 MODEL

To completely avoid the problems arising from the elementary Higgs field in the SM, various kinds of dynamical electroweak symmetry breaking (EWSB) models have been proposed, among which the topcolor scenario is attractive because it can explain the large top quark mass and provide a possible EWSB mechanism [9]. Almost all of these kinds of models propose that the underlying interactions, topcolor interactions, should be flavor nonuniversal. These non-universal interactions in the mass eigenstate basis generate tree-level flavor changing (FC) couplings and result in a rich phenomenology.

A key feature of the TC2 model is the presence of top-pions ( $\pi_t^{0,\pm}$ ), the non-universal gauge boson ( $Z'$ ) and the top-Higgs ( $h_t^0$ ). These new particles treat the third-generation fermions differently from those in the first and second generations and thus can lead to tree-level flavor changing (FC) couplings. When one writes the non-universal interactions in the quark mass eigen-basis, the FC couplings of top-pions to quarks can be written as [10, 11]:

$$\frac{m_t^*}{\sqrt{2}F_\pi} \frac{\sqrt{\nu_w^2 - F_\pi^2}}{\nu_w} \left[ iK_{UR}^{tc} K_{UL}^{tt*} \bar{t}_L c_R \pi_t^0 + \sqrt{2}K_{UR}^{tc*} K_{DL}^{bb} \bar{c}_R b_L \pi_t^+ + \sqrt{2}K_{UR}^{tc} K_{DL}^{bb*} \bar{b}_L c_R \pi_t^- \right. \\ \left. + \sqrt{2}K_{UR}^{tc*} K_{DL}^{ss} \bar{t}_R s_L \pi_t^+ + \sqrt{2}K_{UR}^{tc} K_{DL}^{ss*} \bar{s}_L t_R \pi_t^- \right]. \quad (2)$$

Here  $\nu_w = \nu/\sqrt{2} = 174$  GeV,  $F_\pi \approx 50$  GeV is the top-pion decay constant,  $K_{UL(R)}$  and  $K_{DL(R)}$  are rotation matrices and satisfy the equations  $K_{UL}^+ M_U K_{UR} = M_U^{dia}$  and  $K_{DL}^+ M_D K_{DR} = M_D^{dia}$ , in which  $M_U$  and  $M_D$  are up-quark and down-quark mass matrices, respectively. The values of the coupling parameters can be taken as [10]:

$$K_{UL}^{tt} \approx K_{DL}^{bb} \approx K_{DL}^{ss} \approx 1, \quad K_{UR}^{tc} \leq \sqrt{2\varepsilon - \varepsilon^2}. \quad (3)$$

In our numerical analysis, we will take  $K_{UR}^{tc} = \sqrt{2\varepsilon - \varepsilon^2}$ . The predicted top-Higgs  $h_t^0$  is a  $t\bar{t}$  bound analogous to the  $\sigma$  particle in low energy QCD, and its Feynman rules are similar to the SM Higgs boson.

The Flavor diagonal (FD) couplings of top-pions to fermions take the form [9, 12]:

$$\begin{aligned} & \frac{m_t^*}{\sqrt{2}F_\pi} \frac{\sqrt{\nu_w^2 - F_\pi^2}}{\nu_w} \left[ i\bar{t}\gamma^5 t\pi_t^0 + \sqrt{2}\bar{t}_R b_L \pi_t^+ + \sqrt{2}\bar{b}_L t_R \pi_t^- \right] \\ & + \frac{m_b^*}{\sqrt{2}F_\pi} \left[ i\bar{b}\gamma^5 b\pi_t^0 + \sqrt{2}\bar{t}_L b_R \pi_t^+ + \sqrt{2}\bar{b}_R t_L \pi_t^- \right] + \frac{m_l}{\nu} \bar{l}\gamma^5 l\pi_t^0. \end{aligned} \quad (4)$$

The TC2 model postulates that topcolor interactions mainly couple to the third generation fermions, and give rise to the main part of the quark mass  $m_t^* = m_t(1 - \varepsilon)$ , while the masses of the ordinary fermions are induced by ETC (extended technicolor) interactions with  $m_b^* = m_b - 0.1\varepsilon m_t$ .

The FC couplings of the non-universal gauge boson  $Z'$  to fermions, which may provide significant contributions to some FCNC processes, can be written as [13]:

$$\mathcal{L}_{Z'}^{FC} = -\frac{g_1}{2} \cot \theta' Z'^\mu \left\{ \frac{1}{3} D_L^{bb} D_L^{bs*} \bar{s}_L \gamma_\mu b_L - \frac{2}{3} D_R^{bb} D_R^{bs*} \bar{s}_R \gamma_\mu b_R + \text{h.c.} \right\}, \quad (5)$$

Here  $g_1$  is the ordinary hypercharge gauge coupling constant,  $D_L, D_R$  are matrices which rotate the weak eigen-basis to the mass eigen-basis for the down-type left and right hand quarks. The FD couplings of  $Z'$  to fermions can be written as [9, 11, 12]:

$$\begin{aligned} \mathcal{L}_{Z'}^{FD} = & -\sqrt{4\pi K_1} \left\{ Z'_\mu \left[ \frac{1}{2} \bar{t}_L \gamma^\mu \tau_L - \bar{t}_R \gamma^\mu \tau_R + \frac{1}{6} \bar{t}_L \gamma^\mu t_L + \frac{1}{6} \bar{b}_L \gamma^\mu b_L + \frac{2}{3} \bar{t}_R \gamma^\mu t_R \right. \right. \\ & \left. \left. - \frac{1}{3} \bar{b}_R \gamma^\mu b_R \right] - \tan^2 \theta' Z'_\mu \left[ \frac{1}{6} \bar{s}_L \gamma^\mu s_L - \frac{1}{3} \bar{s}_R \gamma^\mu s_R - \frac{1}{2} \bar{\mu}_L \gamma^\mu \mu_L - \bar{\mu}_R \gamma^\mu \mu_R \right. \right. \\ & \left. \left. - \frac{1}{2} \bar{e}_L \gamma^\mu e_L - \bar{e}_R \gamma^\mu e_R \right] \right\}. \end{aligned} \quad (6)$$

Here  $\theta'$  is the mixing angle, and  $K_1$  is the coupling constant with  $\tan \theta' = \frac{g_1}{\sqrt{4\pi K_1}}$ .

### III. EFFECTIVE HAMILTONIAN AND FORM FACTORS

In the TC2 model, after neglecting the doubly Cabibbo-suppressed contributions, the effective hamiltonian for the transition  $b \rightarrow sl^+l^-$  has the following structure [14, 15]:

$$\mathcal{H} = -\frac{4G_F}{\sqrt{2}} V_{ts}^* V_{tb} \sum_{i=1}^{10} [C_i(\mu) \mathcal{O}_i(\mu) + C_{Q_i}(\mu) Q_i(\mu)] \quad (7)$$

where  $V_{ts}^* V_{tb}$  is the CKM factor, and  $G_F$  is the Fermi coupling constant.  $C_i$  and  $C_{Q_i}$  are the Wilson coefficients at the renormalization point  $\mu = m_W$ ,  $\mathcal{O}_i$ 's ( $i = 1, \dots, 10$ ) are the operators in the SM and the explicit expressions can be found in Ref. [16], and  $Q_i$ 's come

from the diagrams exchanging the neutral particles in TC2 and are [14, 15]

$$\begin{aligned}
Q_1 &= \frac{e^2}{16\pi^2} (\bar{s}_L^\alpha b_R^\alpha) (\bar{l}l), & Q_2 &= \frac{e^2}{16\pi^2} (\bar{s}_L^\alpha b_R^\alpha) (\bar{l}\gamma_5 l), \\
Q_3 &= \frac{g_s^2}{16\pi^2} (\bar{s}_L^\alpha b_R^\alpha) \left( \sum_q \bar{q}_L^\beta q_R^\beta \right), & Q_4 &= \frac{g_s^2}{16\pi^2} (\bar{s}_L^\alpha b_R^\alpha) \left( \sum_q \bar{q}_R^\beta q_L^\beta \right), \\
Q_5 &= \frac{g_s^2}{16\pi^2} (\bar{s}_L^\alpha b_R^\beta) \left( \sum_q \bar{q}_L^\beta q_R^\alpha \right), & Q_6 &= \frac{g_s^2}{16\pi^2} (\bar{s}_L^\alpha b_R^\beta) \left( \sum_q \bar{q}_R^\beta q_L^\alpha \right), \\
Q_7 &= \frac{g_s^2}{16\pi^2} (\bar{s}_L^\alpha \sigma^{\mu\nu} b_R^\alpha) \left( \sum_q \bar{q}_L^\beta \sigma_{\mu\nu} q_R^\beta \right), & Q_8 &= \frac{g_s^2}{16\pi^2} (\bar{s}_L^\alpha \sigma^{\mu\nu} b_R^\alpha) \left( \sum_q \bar{q}_R^\beta \sigma_{\mu\nu} q_L^\beta \right), \\
Q_9 &= \frac{g_s^2}{16\pi^2} (\bar{s}_L^\alpha \sigma^{\mu\nu} b_R^\beta) \left( \sum_q \bar{q}_L^\beta \sigma_{\mu\nu} q_R^\alpha \right), & Q_{10} &= \frac{g_s^2}{16\pi^2} (\bar{s}_L^\alpha \sigma^{\mu\nu} b_R^\beta) \left( \sum_q \bar{q}_R^\beta \sigma_{\mu\nu} q_L^\alpha \right). \quad (8)
\end{aligned}$$

where  $\alpha$  and  $\beta$  denote color indices. The subscripts  $L$  and  $R$  refer to left- and right-handed components of the fermion fields.  $e$  and  $g_s$  are the electromagnetic and strong coupling constants respectively.

In terms of the above effective Hamiltonian (7), the decay amplitude of  $b \rightarrow sl^+l^-$  can be written as [15]:

$$\begin{aligned}
\mathcal{M} &= \frac{G_F \alpha_{em}}{2\sqrt{2}\pi} V_{tb} V_{ts}^* \left\{ -2\tilde{C}_7^{eff} \hat{m}_b \bar{s}_i \sigma_{\mu\nu} \frac{\hat{q}^\nu}{\hat{s}} (1 + \gamma_5) b \bar{l} \gamma^\mu l + \tilde{C}_9^{eff} \bar{s} \gamma_\mu (1 - \gamma_5) b \bar{l} \gamma^\mu l \right. \\
&\quad \left. + \tilde{C}_{10}^{eff} \bar{s} \gamma_\mu (1 - \gamma_5) b \bar{l} \gamma^\mu \gamma_5 l + C_{Q_1} \bar{s} (1 + \gamma_5) b \bar{l} + C_{Q_2} \bar{s} (1 + \gamma_5) b \bar{l} \gamma_5 l \right\}. \quad (9)
\end{aligned}$$

In the SM, the effective Wilson coefficients which enter the decay distributions are written as [16]

$$C_9^{\text{eff}}(\hat{s}) = C_9 + Y(\hat{s}), \quad (10)$$

in which  $Y(\hat{s})$  stands for the matrix element of four-quark operators and given by

$$\begin{aligned}
Y(\hat{s}) &= h(z, \hat{s}) (3C_1 + C_2 + 3C_3 + C_4 + 3C_5 + C_6) - \frac{1}{2} h(1, \hat{s}) (4C_3 + 4C_4 + 3C_5 + C_6) \\
&\quad - \frac{1}{2} h(0, \hat{s}) (C_3 + 3C_4) + \frac{2}{9} (3C_3 + C_4 + 3C_5 + C_6). \quad (11)
\end{aligned}$$

Here the long-distance contributions from the resonant states have been neglected because they could be excluded by experimental analysis [2]. The detailed discussion of the resonance effects can be found in Ref. [17].

In the TC2 model, After the breaking of the extended gauge group to their diagonal subgroups, the non-universal massive gauge boson  $Z'$  is produced. It generally couples to the third-generation fermions and have large tree-level flavor changing couplings. The

non-universal gauge boson  $Z'$  can give a correction to the function  $C_0(x)$  of the SM [18]. For  $l = e, \mu$ , the  $C_{01}^{TC2}(x)$  is [19]

$$C_{01}^{TC2}(y_t) = \frac{-\tan^2\theta' M_Z^2}{M_{Z'}^2} [K_{ab}(y_t) + K_c(y_t) + K_d(y_t)], \quad (12)$$

with  $y_t = m_t^{*2}/M_W^2$ . For the decay process  $B_s \rightarrow \phi\tau^+\tau^-$ , the factor  $-\tan^2\theta'$  should be replaced by 1. For the convenience of the reader, we present the functions  $K_{ab}(y_t)$ ,  $K_c(y_t)$  and  $K_d(y_t)$  in the Appendix A.

The charged top-pions  $\pi_t^\pm$  can give contributions to the corresponding SM functions  $C_0(x)$ ,  $D_0(x)$ ,  $E_0(x)$  and  $E'_0(x)$ . The explicit expressions of these functions are [20]:

$$C_{02}^{TC2}(z_t) = \frac{m_\pi^2}{4\sqrt{2}G_F M_W^2 F_\pi^2} \left[ -\frac{z_t^2}{8(1-z_t)} - \frac{z_t^2}{8(1-z_t)^2} \log[z_t] \right], \quad (13)$$

$$D_0^{TC2}(z_t) = \frac{1}{4\sqrt{2}G_F F_\pi^2} \left[ \frac{47 - 79z_t + 38z_t^2}{108(1-z_t)^3} + \frac{3 - 6z_t^2 + 4z_t^3}{18(1-z_t)^4} \log[z_t] \right], \quad (14)$$

$$E_0^{TC2}(z_t) = \frac{1}{4\sqrt{2}G_F F_\pi^2} \left[ \frac{7 - 29z_t + 16z_t^2}{36(1-z_t)^3} - \frac{3z_t^2 - 2z_t^3}{6(1-z_t)^4} \log[z_t] \right], \quad (15)$$

$$E'_0{}^{TC2}(z_t) = \frac{1}{8\sqrt{2}G_F F_\pi^2} \left[ -\frac{5 - 19z_t + 20z_t^2}{6(1-z_t)^3} + \frac{z_t^2 - 2z_t^3}{(1-z_t)^4} \log[z_t] \right]. \quad (16)$$

Here  $z_t = m_t^{*2}/m_{\pi_t^\pm}^2$ .

The neutral top-pion  $\pi_t^0$  and top-Higgs  $h_t^0$  can also give contributions to the rare decays  $B_s \rightarrow \phi l^+ l^-$  through the new operators given in Eq. (8) [19]. The corresponding Wilson coefficients are written as:

$$C_{Q_1} = \frac{\sqrt{\nu_w^2 - F_\pi^2}}{\nu_w} \left[ \frac{m_b^* m_l \nu}{2\sqrt{2} \sin^2\theta_w F_\pi m_{\pi_t^0}^2} C_0(x_t) + \frac{V_{ts} m_l m_t^* m_b^{*2} M_W^2}{4\sqrt{2} \nu g_2^4 F_\pi^3 m_{\pi_t^0}^2} C(x_s) \right]. \quad (17)$$

Here  $x_s = m_t^{*2}/m_{\pi_t^0}^2$ ,  $g_2$  is the  $SU(2)$  coupling constant, and  $C_0(x_t)$  is the Inami-Lim function in the SM [18]. The expression of  $C_{Q_2}$  is same as that of  $C_{Q_1}$  except for the masses of the scalar particles.

Exclusive decays are described in terms of matrix elements of the quark operators in Eq. (9) over meson states, which are described by several independent form factors. For  $B_s \rightarrow \phi l^+ l^-$ , the related transition matrix elements are defined as ( $q = p - k$ ) [21]

$$\begin{aligned} \langle \phi(k) | (V - A)_\mu | B(p) \rangle &= -i\epsilon_\mu^*(m_{B_s} + m_\phi) A_1(s) + i(p+k)_\mu (\epsilon^* p) \frac{A_2(s)}{m_{B_s} + m_\phi} \\ &+ iq_\mu (\epsilon^* p) \frac{2m_\phi}{s} (A_3(s) - A_0(s)) + \epsilon_{\mu\nu\rho\sigma} \epsilon^{*\nu} p^\rho k^\sigma \frac{2V(s)}{m_{B_s} + m_\phi}. \end{aligned} \quad (18)$$

TABLE I. Form factors for  $B_s \rightarrow \phi$  transition within the light-cone QCD sum rule.

	$F(0)$	$r_1$	$m_R^2$	$r_2$	$m_{\text{fit}}^2$
$V^{B_s \rightarrow \phi}$	0.434	1.484	5.32 <sup>2</sup>	-1.049	39.52
$A_0^{B_s \rightarrow \phi}$	0.474	3.310	5.28 <sup>2</sup>	-2.835	31.57
$A_1^{B_s \rightarrow \phi}$	0.311	—	—	0.308	36.54
$A_2^{B_s \rightarrow \phi}$	0.234	-0.054	—	0.288	48.94
$T_1^{B_s \rightarrow \phi}$	0.349	1.303	5.32 <sup>2</sup>	-0.954	38.28
$T_2^{B_s \rightarrow \phi}$	0.349	—	—	0.349	37.21
$\tilde{T}_3^{B_s \rightarrow \phi}$	0.349	0.027	—	0.321	45.56

with  $A_3(s) = \frac{m_{B_s} + m_\phi}{2m_\phi} A_1(s) - \frac{m_{B_s} - m_\phi}{2m_\phi} A_2(s)$  and  $A_0(0) = A_3(0)$ ,

$$\begin{aligned}
\langle \phi(k) | \bar{s} \sigma_{\mu\nu} q^\nu (1 + \gamma_5) b | B(p) \rangle &= i \epsilon_{\mu\nu\rho\sigma} \epsilon^{*\nu} p^\rho k^\sigma 2T_1(s) \\
&+ T_2(s) \{ \epsilon_\mu^* (m_{B_s}^2 - m_\phi^2) - (\epsilon^* k)_\mu (p + k)_\mu \} \\
&+ T_3(s) (\epsilon^* p) \left\{ q_\mu - \frac{s}{m_{B_s}^2 - m_\phi^2} (p + k)_\mu \right\}. \quad (19)
\end{aligned}$$

with  $T_1(0) = T_2(0)$ .  $\epsilon_\mu$  is the polarization vector of the  $\phi$  meson. The physical range in  $s = q^2$  extends from  $s_{\text{min}} = 0$  to  $s_{\text{max}} = (m_{B_s} - m_\phi)^2$ .

Form factors for  $B_s \rightarrow \phi$  transition have been updated recently in the light-cone QCD sum rule approach [21]. For the  $q^2$  dependence of the form factors, they have been parameterized by a simple formulae with two or three parameters. The form factors  $V$ ,  $A_0$  and  $T_1$  are parameterized by

$$F(s) = \frac{r_1}{1 - s/m_R^2} + \frac{r_2}{1 - s/m_{\text{fit}}^2}, \quad (20)$$

For the form factors  $A_2$  and  $\tilde{T}_3$ , it can be expanded to the second order around the pole, giving

$$F(s) = \frac{r_1}{1 - s/m^2} + \frac{r_2}{(1 - s/m)^2}, \quad (21)$$

where  $m = m_{\text{fit}}$  for  $A_2$  and  $\tilde{T}_3$ . The fit formula for  $A_1$  and  $T_2$  is

$$F(s) = \frac{r_2}{1 - s/m_{\text{fit}}^2}. \quad (22)$$

The form factor  $T_3$  can be obtained by  $T_3(s) = \frac{m_{B_s}^2 - m_\phi^2}{s} [\tilde{T}_3(s) - T_2(s)]$ . All of the form factors are collected Table I.

#### IV. BASIC FORMULA FOR OBSERVABLES

In this section, we give formula for experimental observables including dilepton invariant mass spectrum, forward-backward asymmetry (FBA), and lepton polarization.

From Eqs. (9-19), the decay matrix element of  $B_s \rightarrow \phi l^+ l^-$  can be written in the form

$$\mathcal{M} = -\frac{G_F \alpha_{em}}{2\sqrt{2}\pi} V_{tb} V_{ts}^* m_{B_s} [\mathcal{T}_\mu^1(\bar{l}\gamma^\mu l) + \mathcal{T}_\mu^2(\bar{l}\gamma^\mu \gamma_5 l) + \mathcal{S}(\bar{l}l)] \quad (23)$$

with

$$\mathcal{T}_\mu^1 = A(\hat{s}) \epsilon_{\mu\rho\alpha\beta} \epsilon^{*\rho} \hat{p}^\alpha \hat{k}^\beta - iB(\hat{s}) \epsilon_\mu^* + iC(\hat{s}) (\epsilon^* \cdot \hat{p})(\hat{p} + \hat{k})_\mu, \quad (24)$$

$$\mathcal{T}_\mu^2 = E(\hat{s}) \epsilon_{\mu\rho\alpha\beta} \epsilon^{*\rho} \hat{p}^\alpha \hat{k}^\beta - iF(\hat{s}) \epsilon_\mu^* + iG(\hat{s}) (\epsilon^* \cdot \hat{p})(\hat{p} + \hat{k})_\mu + iH(\hat{s}) (\epsilon^* \cdot \hat{p}) \hat{q}_\mu, \quad (25)$$

$$\mathcal{S} = i2\hat{m}_\phi (\epsilon^* \cdot \hat{p}) \mathcal{S}_2(\hat{s}) \quad (26)$$

where  $\hat{m} = \frac{m}{m_{B_s}}$ ,  $\hat{p} = \frac{p}{m_{B_s}}$ , and the auxiliary functions are then given by:

$$A(\hat{s}) = \frac{2}{1 + \hat{m}_\phi} \tilde{C}_9^{eff}(\hat{s}) V(\hat{s}) + \frac{4\hat{m}_b}{\hat{s}} \tilde{C}_7^{eff} T_1(\hat{s}), \quad (27)$$

$$B(\hat{s}) = (1 + \hat{m}_\phi) \tilde{C}_9^{eff}(\hat{s}) A_1(\hat{s}) + \frac{2\hat{m}_b}{\hat{s}} (1 - \hat{m}_\phi^2) \tilde{C}_7^{eff} T_2(\hat{s}), \quad (28)$$

$$C(\hat{s}) = \frac{1}{1 + \hat{m}_\phi} \tilde{C}_9^{eff}(\hat{s}) A_2(\hat{s}) + \frac{2\hat{m}_b}{1 - \hat{m}_\phi^2} \tilde{C}_7^{eff} \left( T_3(\hat{s}) + \frac{1 - \hat{m}_\phi^2}{\hat{s}} T_2(\hat{s}) \right), \quad (29)$$

$$E(\hat{s}) = \frac{2}{1 + \hat{m}_\phi} \tilde{C}_{10}^{eff} V(\hat{s}), \quad (30)$$

$$F(\hat{s}) = (1 + \hat{m}_\phi) \tilde{C}_{10}^{eff} A_1(\hat{s}), \quad (31)$$

$$G(\hat{s}) = \frac{1}{1 + \hat{m}_\phi} \tilde{C}_{10}^{eff} A_2(\hat{s}), \quad (32)$$

$$H(\hat{s}) = \frac{2\hat{m}_\phi}{\hat{s}} \tilde{C}_{10}^{eff} (A_3(\hat{s}) - A_0(\hat{s})) + \frac{\hat{m}_\phi}{\hat{m}_l(\hat{m}_b + \hat{m}_s)} C_{Q_2} A_0(\hat{s}), \quad (33)$$

$$\mathcal{S}_2(\hat{s}) = -\frac{1}{(\hat{m}_b + \hat{m}_s)} A_0(\hat{s}) C_{Q_1}. \quad (34)$$

The contributions of  $Z'$  and charged top-pions are translated through the RGE step into modifications of the effective Wilson coefficients  $\tilde{C}_7^{eff}$ ,  $\tilde{C}_9^{eff}$  and  $\tilde{C}_{10}^{eff}$ , while the contributions of neutral top-pion and top-Higgs are incorporated in the terms of  $H(\hat{s})$  and  $\mathcal{S}_2(\hat{s})$ .

The two kinematic variables  $\hat{s}$  and  $\hat{u}$  are chosen to be

$$\hat{s} = \hat{q}^2 = (\hat{p}_+ + \hat{p}_-)^2, \quad (35)$$

$$\hat{u} = (\hat{p} - \hat{p}_-)^2 - (\hat{p} - \hat{p}_+)^2, \quad (36)$$



which are bounded as

$$(2\hat{m}_l)^2 \leq \hat{s} \leq (1 - \hat{m}_\phi)^2, \quad (37)$$

$$-\hat{u}(\hat{s}) \leq \hat{u} \leq \hat{u}(\hat{s}), \quad (38)$$

with  $\hat{m}_l = m_l/m_B$ . Here the variable  $\hat{u}$  is related to the angle  $\theta$  between the momentum of the  $B$ -meson and that of  $l^+$  in the center of mass frame of the dileptons  $l^+l^-$  through the relation  $\hat{u} = -\hat{u}(\hat{s}) \cos \theta$ .  $\hat{u}(\hat{s})$  can be written as follows

$$\hat{u}(\hat{s}) = \sqrt{\lambda(1 - 4\frac{\hat{m}_l^2}{\hat{s}})}, \quad (39)$$

with

$$\begin{aligned} \lambda &\equiv \lambda(1, \hat{m}_\phi^2, \hat{s}) \\ &= 1 + \hat{m}_\phi^4 + \hat{s}^2 - 2\hat{s} - 2\hat{m}_\phi^2(1 + \hat{s}). \end{aligned} \quad (40)$$

Keeping the lepton mass and integrating over  $\hat{u}$  in the kinematic region given in Eq. (38), we can obtain the differential decay rates for the decays  $B_s \rightarrow \phi l^+ l^-$ :

$$\frac{dBr}{d\hat{s}} = \tau_{B_s} \frac{G_F^2 \alpha_{em}^2 m_{B_s}^5}{2^{10} \pi^5} |V_{tb} V_{ts}^*|^2 \hat{u}(\hat{s}) D^\phi, \quad (41)$$

$$\begin{aligned} D^\phi &= \frac{|A|^2}{3} \hat{s} \lambda (1 + 2\frac{\hat{m}_l^2}{\hat{s}}) + \frac{|E|^2}{3} \hat{s} \hat{u}(\hat{s})^2 + |\mathcal{S}_2|^2 (\hat{s} - 4\hat{m}_l^2) \lambda \\ &+ \frac{1}{4\hat{m}_\phi^2} \left[ |B|^2 \left( \lambda - \frac{\hat{u}(\hat{s})^2}{3} + 8\hat{m}_\phi^2 (\hat{s} + 2\hat{m}_l^2) \right) + |F|^2 \left( \lambda - \frac{\hat{u}(\hat{s})^2}{3} + 8\hat{m}_\phi^2 (\hat{s} - 4\hat{m}_l^2) \right) \right] \\ &+ \frac{\lambda}{4\hat{m}_\phi^2} \left[ |C|^2 \left( \lambda - \frac{\hat{u}(\hat{s})^2}{3} \right) + |G|^2 \left( \lambda - \frac{\hat{u}(\hat{s})^2}{3} + 4\hat{m}_l^2 (2 + 2\hat{m}_\phi^2 - \hat{s}) \right) \right] \\ &- \frac{1}{2\hat{m}_\phi^2} \left[ Re(BC^*) (1 - \hat{m}_\phi^2 - \hat{s}) \left( \lambda - \frac{\hat{u}(\hat{s})^2}{3} \right) \right. \\ &\left. + Re(FG^*) \left( (1 - \hat{m}_\phi^2 - \hat{s}) \left( \lambda - \frac{\hat{u}(\hat{s})^2}{3} \right) + 4\hat{m}_l^2 \lambda \right) \right] \\ &- 2\frac{\hat{m}_l^2}{\hat{m}_\phi^2} \lambda [Re(FH^*) - Re(GH^*) (1 - \hat{m}_\phi^2)] + |H|^2 \frac{\hat{m}_l^2}{\hat{m}_\phi^2} \hat{s} \lambda \end{aligned} \quad (42)$$

The normalized forward-backward asymmetries (FBA) is defined as

$$\mathcal{A}_{FB}(\hat{s}) = \int d\hat{s} \frac{\int_{-1}^{+1} d\cos\theta \frac{d^2 Br}{d\hat{s} d\cos\theta} \text{Sign}(\cos\theta)}{\int_{-1}^{+1} d\cos\theta \frac{d^2 Br}{d\hat{s} d\cos\theta}}. \quad (43)$$

According to this definition, the explicit expressions of FBA for the exclusive decays is:

$$\begin{aligned} \frac{d\mathcal{A}_{FB}}{d\hat{s}} &= \frac{1}{D^\phi} \hat{u}(\hat{s}) \left\{ \hat{s} [Re(BE^*) + Re(AF^*)] \right. \\ &\left. + \frac{\hat{m}_l}{\hat{m}_\phi} [Re(\mathcal{S}_2 B^*) (1 - \hat{s} - \hat{m}_\phi^2) - Re(\mathcal{S}_2 C^*) \lambda] \right\}. \end{aligned} \quad (44)$$

Now we are ready to present the analytical expressions of lepton polarization by defining:

$$\frac{d\Gamma(\hat{n})}{d\hat{s}} = \frac{1}{2} \left( \frac{d\Gamma}{d\hat{s}} \right)_0 [1 + (P_L \hat{e}_L + P_N \hat{e}_N + P_T \hat{e}_T) \cdot \hat{n}] \quad (45)$$

where the subscript "0" corresponds to the unpolarized decay case,  $P_L$  and  $P_T$  are the longitudinal and transverse polarization asymmetries in the decay plane respectively, and  $P_N$  is the normal polarization asymmetry in the direction perpendicular to the decay plane.

The lepton polarization asymmetry  $P_i$  can be derived by

$$P_i(\hat{s}) = \frac{d\Gamma(\hat{n} = \hat{e}_i)/d\hat{s} - d\Gamma(\hat{n} = -\hat{e}_i)/d\hat{s}}{d\Gamma(\hat{n} = \hat{e}_i)/d\hat{s} + d\Gamma(\hat{n} = -\hat{e}_i)/d\hat{s}} \quad (46)$$

the results are

$$P_L = \frac{1}{D^\phi} \mathcal{D} \left\{ \frac{2\hat{s}\lambda}{3} \text{Re}(AE^*) + \frac{(\lambda + 12\hat{s}\hat{m}_\phi^2)}{3\hat{m}_\phi^2} \text{Re}(BF^*) \right. \\ \left. - \frac{\lambda(1 - \hat{m}_\phi^2 - \hat{s})}{3\hat{m}_\phi^2} \text{Re}(BG^* + CF^*) + \frac{\lambda^2}{3\hat{m}_\phi} \text{Re}(CG^*) \right. \\ \left. + \frac{2\hat{m}_l\lambda}{\hat{m}_\phi} [\text{Re}(FS_2^*) - \hat{s}\text{Re}(HS_2^*) - (1 - \hat{m}_\phi^2)\text{Re}(GS_2^*)] \right\}, \quad (47)$$

$$P_N = \frac{1}{D^\phi} \frac{-\pi\sqrt{\hat{s}}\hat{u}(\hat{s})}{4\hat{m}_\phi} \left\{ \frac{\hat{m}_l}{\hat{m}_\phi} [ \text{Im}(FG^*)(1 + 3\hat{m}_\phi^2 - \hat{s}) \right. \\ \left. + \text{Im}(FH^*)(1 - \hat{m}_\phi^2 - \hat{s}) - \text{Im}(GH^*)\lambda ] \right. \\ \left. + 2\hat{m}_\phi\hat{m}_l [\text{Im}(BE^*) + \text{Im}(AF^*)] \right. \\ \left. - (1 - \hat{m}_\phi^2 - \hat{s})\text{Im}(BS_2^*) + \lambda\text{Im}(CS_2^*) \right\}, \quad (48)$$

$$P_T = \frac{1}{D^\phi} \frac{\pi\sqrt{\lambda}\hat{m}_l}{4\sqrt{\hat{s}}} \left\{ 4\hat{s}\text{Re}(AB^*) \right. \\ \left. + \frac{(1 - \hat{m}_\phi^2 - \hat{s})}{\hat{m}_\phi^2} [-\text{Re}(BF^*) + (1 - \hat{m}_\phi^2)\text{Re}(BG^*) + \hat{s}\text{Re}(BH^*)] \right. \\ \left. + \frac{\lambda}{\hat{m}_\phi^2} [\text{Re}(CF^*) - (1 - \hat{m}_\phi^2)\text{Re}(CG^*) - \hat{s}\text{Re}(CH^*)] \right. \\ \left. + \frac{(\hat{s} - 4\hat{m}_l^2)}{\hat{m}_\phi\hat{m}_l} [(1 - \hat{m}_\phi^2 - \hat{s})\text{Re}(FS_2^*) - \lambda\text{Re}(GS_2^*)] \right\}. \quad (49)$$

where  $\mathcal{D} = \sqrt{1 - 4\frac{\hat{m}_t^2}{\hat{s}}}$ ,  $D^\phi$  are given in Eq. (42).

## V. NUMERICAL RESULT

In the numerical calculations, we fix the SM parameters as follows [22–24].

$$\begin{aligned}
A &= 0.8095, \quad \lambda = 0.22545, \quad \bar{\rho} = 0.132 \pm 0.02, \quad \bar{\eta} = 0.367 \pm 0.013. \\
m_c &= 1.4 \text{ GeV}, \quad m_b = 4.8 \text{ GeV}, \quad m_t = 172.4 \text{ GeV}, \\
m_\mu &= 0.1057 \text{ GeV}, \quad m_\tau = 1.7769 \text{ GeV}, \quad m_W = 80.4 \text{ GeV}, \\
m_Z &= 91.18 \text{ GeV}, \quad m_{B_s} = 5.36 \text{ GeV}, \quad m_\phi = 1.02 \text{ GeV}, \\
\alpha_{em} &= \frac{1}{137}, \quad \alpha_s(m_Z) = 0.118, \quad \sin^2\theta_W = 0.23, \quad \tau_{B_s} = 1.46 \times 10^{-12} \text{ s}. \quad (50)
\end{aligned}$$

In the TC2 model, the new physics contributions depend on new parameters which have been constrained by theory arguments and by experimental results.  $\varepsilon$  denotes the portion of the top quark mass generated by the extended technicolor. The experimental constraints on  $\varepsilon$  from the data of radiative decay  $b \rightarrow s\gamma$  are weak [25]. However, from the theoretical point of view,  $\varepsilon$  is favored in the range of [0.03, 0.1] [9].

On the theoretical side, Ref. [9] estimated that the mass of top-pions should be a few hundred GeV using quark loop approximation, and Refs. [9, 10] evaluated the mass of top-Higgs to be about  $2m_t$ . On the experimental side, the neutral top-pion and the top-Higgs are weakly restricted. Meanwhile, the mass of the charged top-pion have been strongly constrained. For example, the absence of  $t \rightarrow \pi_t^+ b$  indicates that  $m_{\pi_t^+} > 165 \text{ GeV}$  [26], and the analysis of  $R_b$  reveals that  $m_{\pi_t^+} > 220 \text{ GeV}$  [27, 28].

As for the bounds on the mass of  $Z'$ , precision electroweak data show that  $m_{Z'}$  must be larger than 1 TeV [29]. The vacuum tilting, the confinement from Z-pole physics, and U(1) triviality need  $K_1 \leq 1$  [30]. When considering experimentally much better measured modes such as  $B \rightarrow \mu^+\mu^-$  and  $B \rightarrow Kl^+l^-$ , we can easily obtain the constraints on the free parameters  $m_{Z'}$  and  $K_1$ . For example, for  $K_1 = 0.4$ , we must have  $1290 \text{ GeV} < m_{Z'} < 1787 \text{ GeV}$  [19].

The differential branching fraction of exclusive decay  $B \rightarrow K^*\mu^+\mu^-$  has been already measured by BaBar, Belle, CDF and LHCb. The latest LHCb result which corresponds to an integrated luminosity of  $1 \text{ fb}^{-1}$  in the low  $q^2$  region is [31]

$$\left[ \frac{dBr}{dq^2}(B \rightarrow K^*\mu^+\mu^-) \right]_{[1,6]} = (0.42 \pm 0.04 \pm 0.04) \times 10^{-7} c^4 / \text{GeV}^2. \quad (51)$$

With the above precise measurement, we give the plots of differential branching fraction  $dBr/dq^2(B \rightarrow K^*\mu^+\mu^-)$  at low  $q^2$  in function of the mass  $M_{Z'}$  (left panel) and of the

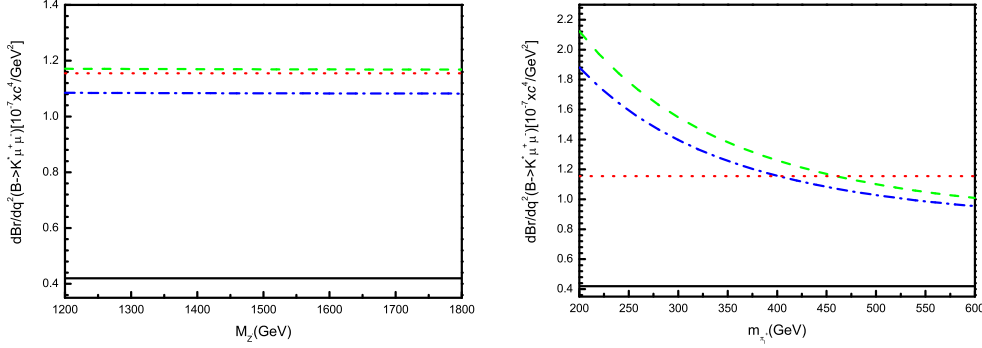


FIG. 1. Plots of differential branching fractions  $dBr/dq^2(B \rightarrow K^*\mu^+\mu^-)$  at low  $q^2$  in function of the mass  $M_{Z'}$  (left panel) and of the mass  $m_{\pi_t^+}$  (right panel).

mass  $m_{\pi_t^+}$  (right panel) in Fig. 1. The solid lines denote the LHCb central value, while the dotted lines show the  $3\sigma$  bound including the experimental errors with theoretical ones given in Table 5 of Ref. [32] (added in quadrature). The dashed and dash-dotted curve corresponds to the TC2 prediction for  $\varepsilon = 0.04$  and  $\varepsilon = 0.08$ , respectively. It is easy to see that the whole parameter space of  $M_{Z'}$  is excluded for  $\varepsilon = 0.04$ , but allowed for  $\varepsilon = 0.08$  by this differential branching fraction. The mass of top-pion  $\pi_t^+$  below 450 GeV for  $\varepsilon = 0.04$  and below 400 GeV for  $\varepsilon = 0.08$  are also excluded by the LHCb data.

After taking into account the new constraints from  $B \rightarrow K^*\mu^+\mu^-$  decay, we will make numerical calculations by using the input parameters in the following ranges:

$$\begin{aligned}
 m_{\pi_t^+} &= (350 - 600)\text{GeV}, & m_{\pi_t^0} &= m_{h_t^0} = (200 - 500)\text{GeV}, & m_{Z'} &= (1200 - 1800)\text{GeV}, \\
 \varepsilon &= (0.06 - 0.1), & K_1 &= (0.3 - 1), & F_\pi &= 50\text{GeV}.
 \end{aligned}
 \tag{52}$$

Using the above input parameters, we will calculate the physics observables as defined in previous sections and study the sensitivity to the new physics corrections appeared in the TC2 model. The invariant mass spectra and branching ratios are almost the same for electron and muon modes because the mass of electron and muon are small. Meanwhile, the electron polarization is very difficult to measure, so we only consider  $B_s \rightarrow \phi\mu^+\mu^-, \phi\tau^+\tau^-$  decays in this work.

Using Eq. (41) and the input parameters as given above, it is easy to calculate the branching ratio  $Br(B_s \rightarrow \phi\mu^+\mu^-, \phi\tau^+\tau^-)$ . In the SM, the numerical results are

$$\begin{aligned}
 Br(B_s \rightarrow \phi\mu^+\mu^-) &= 1.54_{-0.25}^{+0.28} \times 10^{-6}, \\
 Br(B_s \rightarrow \phi\tau^+\tau^-) &= 1.65_{-0.28}^{+0.30} \times 10^{-7}.
 \end{aligned}
 \tag{53}$$

where the error corresponds to the uncertainty of input parameters of form factors.

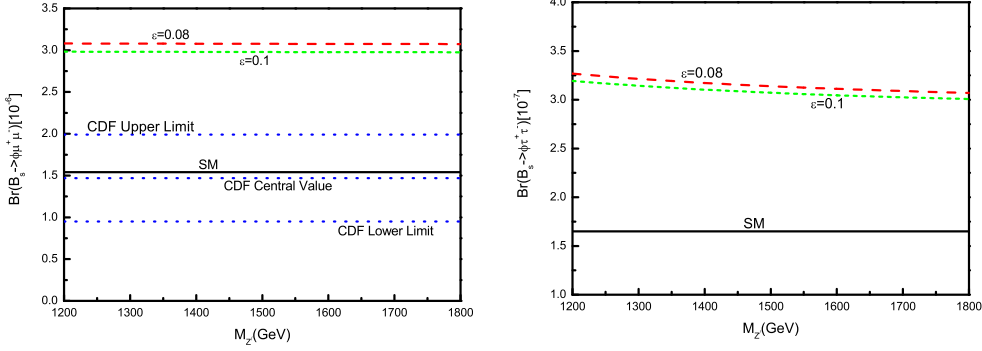


FIG. 2. Plots of branching ratios of  $Br(B_s \rightarrow \phi \mu^+ \mu^-, \phi \tau^+ \tau^-)$  decays versus  $M_{Z'}$  in the SM and TC2 model. The dashed, short-dashed lines and solid curve correspond to the TC2 and SM results, respectively. The dotted lines denote the CDF data with  $1\sigma$  error:  $Br(B_s \rightarrow \phi \mu^+ \mu^-) = (1.47 \pm 0.52) \times 10^{-6}$ .

In the TC2 model, both the new penguin and tree level diagrams contribute through constructive interference with their SM counterparts and consequently provide large enhancements with respect to the SM predictions. For the typical values of  $F_\pi = 50 GeV$ ,  $\varepsilon = 0.08$ ,  $K_1 = 0.4$ ,  $m_{\pi_t^+} = 450 GeV$ ,  $m_{\pi_t^0} = m_{h_t^0} = 300 GeV$  and  $M_{Z'} = 1500 GeV$ , one has

$$Br(B_s \rightarrow \phi \mu^+ \mu^-) = \begin{cases} 1.55 \times 10^{-6} & \text{only } Z' \text{ considered,} \\ 3.07 \times 10^{-6} & \text{only } \pi_t^+ \text{ considered,} \\ 3.76 \times 10^{-6} & \text{both } Z' \text{ and } \pi_t^+ \text{ considered.} \end{cases} \quad (54)$$

$$Br(B_s \rightarrow \phi \tau^+ \tau^-) = \begin{cases} 1.80 \times 10^{-7} & \text{only } Z' \text{ considered,} \\ 2.92 \times 10^{-7} & \text{only } \pi_t^+ \text{ considered,} \\ 3.14 \times 10^{-7} & \text{both } Z' \text{ and } \pi_t^+ \text{ considered.} \end{cases} \quad (55)$$

In Fig. 2, we show the branching ratios of decays  $B_s \rightarrow \phi \mu^+ \mu^-, \phi \tau^+ \tau^-$  as a function of the mass parameter  $M_{Z'}$  in the SM and TC2 model. The solid line refers to the SM prediction, while the dashed, short-dashed curves correspond to theoretical prediction with the inclusion of the new physics effects of the TC2 model for  $\varepsilon = 0.08$  and  $\varepsilon = 0.1$ , respectively. The dotted lines denote the CDF data with  $1\sigma$  error. From this figure, we can see that the new physics enhancements can be significant in size. For  $B_s \rightarrow \phi \mu^+ \mu^-$  decay mode, the values of branching ratio basically remain unchanged within the range of  $M_{Z'} = 1200 \sim 1800 GeV$ . The theoretical predictions of  $Br(B_s \rightarrow \phi \tau^+ \tau^-)$  have some sensitivity to the parameter  $M_{Z'}$  because the nonuniversal gauge boson  $Z'$  has large couplings to the third generation fermion with respect to the first two generations.

In Fig. 3, we show the branching ratios of decays  $B_s \rightarrow \phi \mu^+ \mu^-, \phi \tau^+ \tau^-$  as a function of the mass parameter  $m_{\pi_t^+}$  in the SM and TC2 model. One can see from Fig. 3 that the new

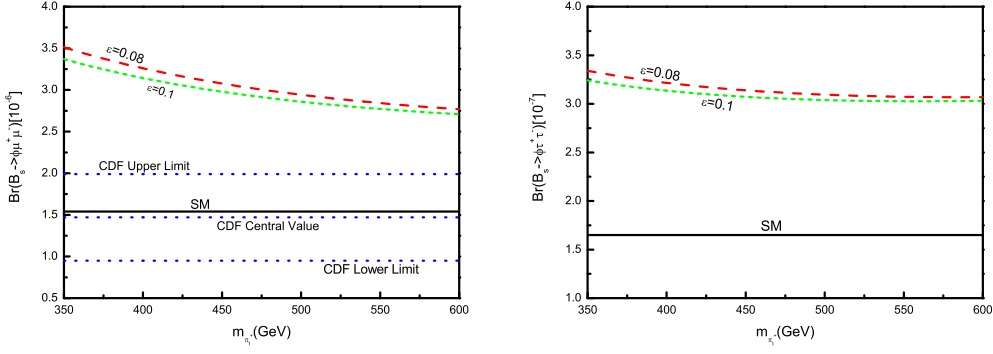


FIG. 3. Plots of branching ratios of  $Br(B_s \rightarrow \phi\mu^+\mu^-, \phi\tau^+\tau^-)$  decays versus  $m_{\pi_t^+}$  in the SM and TC2 model. The dashed, short-dashed lines and solid curve represent the TC2 and SM results, respectively.

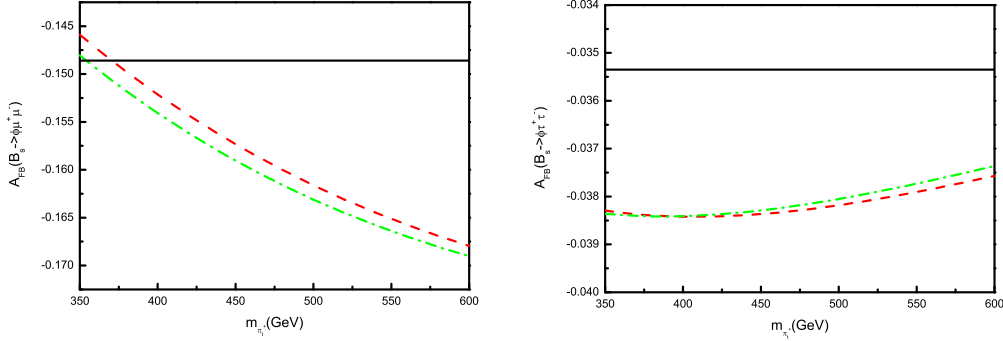


FIG. 4. Plots of forward-backward asymmetries of  $A_{FB}(B_s \rightarrow \phi\mu^+\mu^-, \phi\tau^+\tau^-)$  decays versus  $m_{\pi_t^+}$  in the SM and TC2 model. The dashed, dash-dotted lines and solid curve stand for the TC2 and SM results, respectively.

physics enhancements to the two studied decays are still large in size when the parameter  $m_{\pi_t^+}$  varies. The branching ratios  $Br(B_s \rightarrow \phi\mu^+\mu^-, \phi\tau^+\tau^-)$  are not very sensitive to the variations of the input parameter  $\varepsilon$ . For  $\varepsilon = 0.08$  and  $\varepsilon = 0.1$ , the enhancement to the  $Br(B_s \rightarrow \phi\mu^+\mu^-, \phi\tau^+\tau^-)$  can reach a factor of  $\sim 2$ . The uncertainty of the data is still large. Further improvement of the data will be very helpful to test or constrain the parameter  $m_{\pi_t^+}$  in the TC2 model from these decays.

In Fig. 4, we show the forward-backward asymmetries of decays  $B_s \rightarrow \phi\mu^+\mu^-, \phi\tau^+\tau^-$  as a function of the mass parameter  $m_{\pi_t^+}$  in the SM and TC2 model. The solid line denotes the SM prediction, while the dashed, dash-dotted curves correspond to the theoretical prediction of TC2 model for  $\varepsilon = 0.08$  and  $\varepsilon = 0.1$ , respectively. For  $B_s \rightarrow \phi\mu^+\mu^-$  decay, the theoretical prediction of the forward-backward asymmetry in the SM is:  $A_{FB}(B_s \rightarrow$

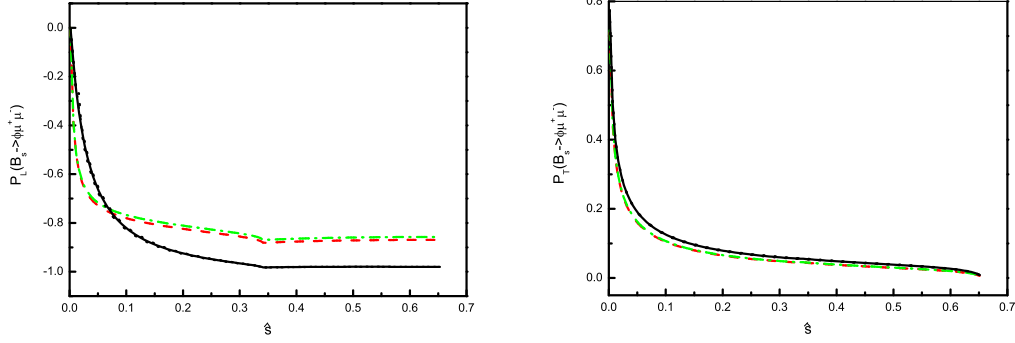


FIG. 5. Plots of  $P_L$  and  $P_T$  for decay  $B_s \rightarrow \phi\mu^+\mu^-$  in the SM and TC2 model. The dashed, dash-dotted lines and solid curve display the central values of the TC2 and SM predictions, respectively. The two dotted lines show the uncertainties of form factors induced by  $F(0)$  in the SM.

$\phi\mu^+\mu^-$ ) =  $-0.149 \pm 0.001$ . In the TC2 model, when the  $\pi_t^+$  mass is in the range of  $350\text{GeV} \sim 600\text{GeV}$ , the value of  $A_{FB}(B_s \rightarrow \phi\mu^+\mu^-)$  is in the range of  $-0.168 \sim -0.146$  for  $\varepsilon = 0.08$ . For  $B_s \rightarrow \phi\tau^+\tau^-$  decay, the forward-backward asymmetry amounts to  $-0.038 \sim -0.037$  for  $\varepsilon = 0.08$ , which is comparable with the SM result of  $-0.035 \pm 0.0001$ .

In Figs. 5 and 6, we present the longitudinal and transverse polarization for decays  $B_s \rightarrow \phi\mu^+\mu^-$  and  $B_s \rightarrow \phi\tau^+\tau^-$ . The solid line is the SM prediction, while the dashed, dash-dotted curves are the theoretical prediction of TC2 model for  $\varepsilon = 0.08$  and  $\varepsilon = 0.1$ , respectively. From these figures, it is easy to see that the variations of the input parameter  $\varepsilon$  can only provide a few percent change of the lepton polarization for  $B_s \rightarrow \phi\mu^+\mu^-$ ,  $\phi\tau^+\tau^-$  decays. For the decay  $B_s \rightarrow \phi\mu^+\mu^-$ , the  $P_L$  is suppressed by about 110% at most at the small momentum transfer, while at  $\hat{s} > 0.07$ , it will become larger than that of the SM, and the new physics contribution in TC2 model provides an enhancement of  $\sim 12\%$ . For the  $P_T$  part, the new physics contribution results in a (8 ~ 18)% decrease. As for  $B_s \rightarrow \phi\tau^+\tau^-$ , the deviation from the SM prediction appears when  $\hat{s} > 0.5$  for  $P_L$ .  $P_T$  is decreased with respect to the SM prediction by about 10% in all the di-lepton invariant mass range. Thus, the measurement of  $P_L$  for  $B_s \rightarrow \phi\mu^+\mu^-$  and  $P_T$  for  $B_s \rightarrow \phi\tau^+\tau^-$  will distinguish between the SM and the TC2 model.

## VI. SUMMARY

In this paper, we carried out a study of the new physics contributions to the branching ratios, forward-backward asymmetries and lepton polarization for the decays  $B_s \rightarrow \phi\mu^+\mu^-$ ,  $\phi\tau^+\tau^-$  in the TC2 model by using form factors calculated within the light-cone

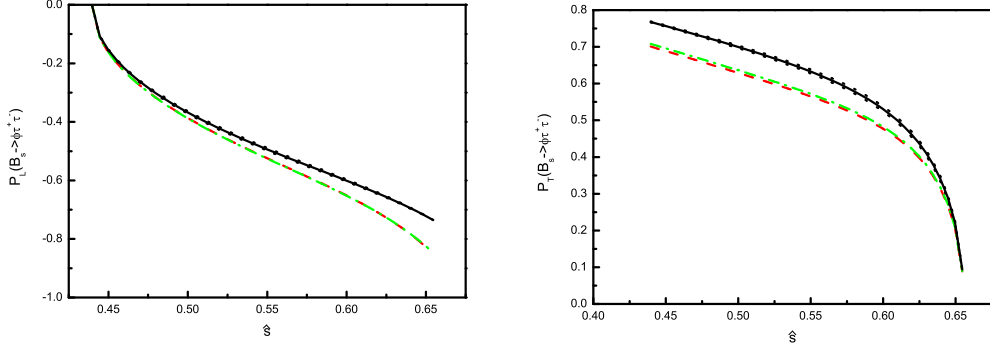


FIG. 6. Plots of  $P_L$  and  $P_T$  for decay  $B_s \rightarrow \phi\tau^+\tau^-$  in the SM and TC2 model. Other captions are same as Fig. 5.

QCD sum rule approach.

In Section II, a brief review about the topcolor-assisted technicolor model was given. In Section III, we presented the theoretical framework for  $B_s \rightarrow \phi l^+ l^-$  decays within the TC2 model, then give the definitions and the derivations of the form factors in the decays  $B_s \rightarrow \phi l^+ l^-$  using the updated form factors within the light-cone QCD sum rule. In Section IV, we introduced the basic formula for experimental observables. In Section V, we calculated the branching ratio, forward-backward asymmetry, and lepton polarization of  $B_s \rightarrow \phi l^+ l^-$  and made phenomenological analysis for these decays in the SM and the TC2 model. From the numerical results, we found the following features about the new physics effects:

- The branching ratios of  $\bar{B}_s \rightarrow \phi\mu^+\mu^-$ ,  $\phi\tau^+\tau^-$  decays are essentially unaffected by the  $Z'$  contributions, while charged top-pions interaction can lead to striking effects in these decay distributions. For  $\varepsilon = 0.08$  and  $\varepsilon = 0.1$ , the enhancement can reach a factor of  $\sim 2$ .
- For the forward-backward asymmetry of the decay  $B_s \rightarrow \phi\mu^+\mu^-$ , the NP enhancement is in the range  $-13\%$  to  $3\%$ . For  $B_s \rightarrow \phi\tau^+\tau^-$  decay, the NP effects is about  $-9\%$  to  $-6\%$  compared to the SM predictions.
- For the lepton polarization,  $P_L(B_s \rightarrow \phi\mu^+\mu^-)$  is increased by about  $12\%$ . However,  $P_T(B_s \rightarrow \phi\mu^+\mu^-)$  is decreased by  $(8 \sim 18)\%$ . As for  $B_s \rightarrow \phi\tau^+\tau^-$ , the deviation from the SM prediction appears when  $\hat{s} > 0.5$  for  $P_L$ . In the  $P_T$  part, the SM prediction will be decreased by about  $10\%$ .

An improved measurement of  $Br(\bar{B}_s \rightarrow \phi\mu^+\mu^-)$  and first measurements of the longi-



tudinal polarization asymmetry,  $P_L$ , in  $B_s \rightarrow \phi\mu^+\mu^-$  and of the transverse polarization asymmetry,  $P_T$ , in  $B_s \rightarrow \phi\tau^+\tau^-$  at LHCb and super-flavor factories (BellIII and the proposed Super-B ) will allow to distinguish between the SM and the TC2 model.

## ACKNOWLEDGMENTS

The authors would like to thank Prof. Zhen-jun Xiao for helpful comments and suggestions on the manuscript. The work is supported by the National Science Foundation under contract No. 10947020, and Natural Science Foundation of Henan Province under Grant No. 112300410188.

## Appendix A: Relevant functions in the TC2 model

In this Appendix, we give the explicit expressions of functions that related to the rare B decays studied here in the framework of the TC2 model.

$$K_{ab}(x) = -\frac{2g^2c_w^2I_1(x)}{3g_2^2(v_d + a_d)}, \quad (\text{A1})$$

$$K_c(x) = \frac{2f^2c_w^2}{g_2^2} \left[ \frac{2I_2(x)}{3(v_u + a_u)} + \frac{I_3(x)}{6(v_u - a_u)} \right], \quad (\text{A2})$$

$$K_d(x) = \frac{2f^2c_w^2}{g_2^2} \left[ \frac{2I_4(x)}{3(v_u + a_u)} + \frac{I_5(x)}{6(v_u - a_u)} \right], \quad (\text{A3})$$

$$C(x) = \frac{I_1(x)}{-[0.5(Q - 1)s_w^2 + 0.25]}. \quad (\text{A4})$$

Here  $g = \sqrt{4\pi K_1}$ ,  $s_w = \sin \theta_w$ ,  $a_{u,d} = I_3$ ,  $v_{u,d} = I_3 - 2Q_{u,d}s_w^2$ , and  $u, d$  stand for the up and down type quarks, respectively.

$$I_1(x) = -(0.5(Q - 1)s_w^2 + 0.25)(x^2\ln(x)/(x - 1)^2 - x/(x - 1) - x(0.5(-0.5772 + \ln(4\pi) - \ln(M_W^2)) + 0.75 - 0.5(x^2\ln(x)/(x - 1)^2 - 1/(x - 1))))), \quad (\text{A5})$$

$$I_2(x) = (0.5Qs_w^2 - 0.25)(x^2\ln(x)/(x - 1)^2 - 2x\ln(x)/(x - 1)^2 + x/(x - 1)), \quad (\text{A6})$$

$$I_3(x) = -Qs_w^2(x/(x - 1) - x\ln(x)/(x - 1)^2), \quad (\text{A7})$$

$$I_4(x) = 0.25(4s_w^2/3 - 1)(x^2\ln(x)/(x - 1)^2 - x - x/(x - 1)), \quad (\text{A8})$$

$$I_5(x) = -0.25Qs_w^2x(-0.5772 + \ln(4\pi) - \ln(M_W^2) + 1 - x\ln(x)/(x - 1) - s_w^2/6(x^2\ln(x)/(x - 1)^2 - x - x/(x - 1))). \quad (\text{A9})$$

- 
- [1] C. Q. Geng, C. C. Liu, J. Phys. G **29**, 1103 (2003).
- [2] CDF Collaboration, “Measurement of forward-backward asymmetry in  $B \rightarrow K^{(*)}\mu^+\mu^-$  and first observation of  $B_s^0 \rightarrow \phi\mu^+\mu^-$ ”, Phys.Rev.Lett. **106**, 161801 (2011) [hep-ex/1001.1028].
- [3] T. Aaltonen *et al.* (CDF Collaboration), Phys. Rev. Lett. **107**, 201802 (2011).
- [4] A. Deandrea, A. D. Polosa, Phys. Rev. D **64**, 074012 (2001).
- [5] G. Erkol, G. Turan, Eur. Phys. J. C **25**, 575 (2002) [hep-ph/0203038].
- [6] R. Mohanta, A. K. Giri, Phys. Rev. D **75**, 035008 (2007) [hep-ph/0611068]; Ying Li, Juan Hua, arXiv:1105.3031 [hep-ph].
- [7] Qin Chang, Yin-Hao Gao, Nucl.Phys. B **845**, 179 (2011) [hep-ph/1101.1272].
- [8] E. Lunghi, A. Soni, JHEP **121**, 1011 (2010) [hep-ph/1007.4015]; S. M. Zebarjad, F. Falahati and H. Mehranfar, Phys. Rev. D **79**, 075006 (2009) [hep-ph/0811.2706]; U. O. Yilmaz, Eur. Phys. J. C **58**, 555 (2008) [hep-ph/0806.0269].
- [9] C. T. Hill, Phys. Lett. B **345**, 483 (1995); K. Lane, T. Eichten, Phys. Lett. B **352**, 382 (1995); K. Lane, Phys. Lett. B **433**, 96 (1998); G. Cvetic, Rev. Mod. Phys. **71**, 513 (1999).
- [10] H. J. He, C. P. Yuan, Phys. Rev. Lett. **83**, 28 (1999); G. Burdman, Phys. Rev. Lett. **83**, 2888 (1999).
- [11] G. Buchalla, G. Burdman, C. T. Hill, D. Kominis, Phys. Rev. D **53**, 5185 (1996).
- [12] C. T. Hill, E. H. Simmons, Phys. Rept. **381**, 235 (2003); **390**, 553(E) (2004).
- [13] C. T. Hill, arXiv:hep-ph/9702320.
- [14] Yuan-Ben Dai, Chao-Shang Huang and Han-Wen Huang, Phys. Lett. B **390**, 257 (1997), Erratum-ibid. B **513**, 429 (2001).
- [15] Wen-jun Li, Yuan-Ben Dai, and Chao-Shang Huang, Eur. Phys. J. C **40** 565 (2005) [hep-ph/0410317].
- [16] A.J. Buras, M. Münz, Phys. Rev. D **52**, 186 (1995).
- [17] M. Beneke, G. Buchalla, M. Neubert, C. T. Sachrajda, Eur. Phys. J. C **61**, 439 (2009) [hep-ph/0902.4446]; M. Bartsch, M. Beylich, G. Buchalla, D. N. Gao, JHEP **0911**, 01 (2009) [hep-ph/0909.1512].
- [18] T. Inami, C. S. Lim, Prog. Theor. Phys. **65**, 297 (1981); A. J. Buras, arXiv:hep-ph/9806471.
- [19] Wei Liu, Chong-xing Yue, and Hui-Di Yang, Phys. Rev. D **79**, 034008 (2009) [hep-ph/0901.3463].
- [20] Z.J. Xiao, W.J. Li, L.B. Guo, G.R. L, Eur. Phys. J. C, **18**, 681 (2001).
- [21] P. Ball and R. Zwicky, Phys. Rev. D **71**, 014029 (2005) [hep-ph/0412079].

- [22] M. Bona *et al.* (UTfit Collaboration) JHEP **0507**, 028 (2005) [hep-ph/0501199]; JHEP **0601** (2006) 081 [hep-ph/0606167]; online update at: <http://www.utfit.org/UTfit/Results>.
- [23] C. Amsler *et al.* (Particle Data Group), J. Phys. G **37**, 075021 (2010).
- [24] Tevatron Electroweak Working Group, CDF Collaboration and D0 Collaboration, arXiv:0808.1089 [hep-ex].
- [25] B. Balaji, Phys. Rev. D **53**, 1699 (1996).
- [26] B. Balaji, Phys. Lett. B **393**, 89 (1997).
- [27] G. Burdman and D. Kominis, Phys. Lett. B **403**, 101 (1997); W. Loinaz and T. Takeuchi, Phys. Rev. D **60**, 015005 (1999).
- [28] C. T. Hill and X. Zhang, Phys. Rev. D **51**, 3563 (1995); C. Yue, Y. P. Kuang, X. Wang and W. Li, Phys. Rev. D **62**, 055005 (2000).
- [29] R. S. Chivukula and E. H. Simmons, Phys. Rev. D **66**, 015006 (2002).
- [30] M. B. Popovic and E. H. Simmons, Phys. Rev. D **58**, 095007 (1998); G. Burdman and N. J. Evens, Phys. Rev. D **59**, 115005 (1999).
- [31] LHCb Collaboration, LHCb-CONF-2012-008, presented at the 47th Rencontres de Moriond on QCD and High Energy Interactions.
- [32] F. Mahmoudi, S. Neshatpour, and J. Orloff, arXiv:1205.1845 [hep-ph].